

Modeling and Analysis of Container-Type Ship's Marine Propeller for Engine Load Conditions

✉ İsmail Çiçek¹, ✉ Naz Yılmaz²

¹Istanbul Technical University Maritime Faculty, Department of Marine Engineering, İstanbul, Türkiye

²Istanbul Technical University Graduate School, Department of Maritime Transportation Engineering, İstanbul, Türkiye

Abstract

Engine room simulators have become increasingly important in practical marine engineering training and education. To ensure their usefulness in both training and academic studies, it is essential to accurately model, simulate, and validate ship propulsion systems within these simulators. This study outlines the design and development of a marine propeller and its hydrodynamic performance analysis using computational fluid dynamics (CFD). To obtain sampled ship and propulsion parameters, a large container-type vessel model in an existing engine room simulator was employed. This study includes the design and development of a new efficient propeller and its propulsion data, which can be used in the development of an engine room simulator. This study demonstrates a methodology for developing training simulators that involve using complex and extensive mathematical modeling. The ship's geometry was designed using 3D modeling software such as Rhinoceros and Maxsurf. To determine the required thrust at each of the main engine's loading modes, the ship's resistance computations were conducted using Maxsurf's HullSpeed module. The authors also developed a MATLAB code to obtain the ship's power requirements. The ship resistance and thrust requirements data were then used as input to design the propeller, and CFD analyses were conducted for the defined engine load conditions. The hydrodynamic performance coefficients of the newly designed propeller were computed, and the CFD results were compared with the existing propeller's performance data. The resulting propulsion data presents the performance parameters for each predefined engine load condition. The analysis demonstrated that a more efficient marine propeller was designed, providing more thrust (up to 9% for a specific mode) while consuming less power compared with the existing one.

Keywords: Propeller design, Container ship, Computational fluid dynamics, Engine load conditions, Engine room simulator

1. Introduction

Since the publication of Standards of Training Certification and Watchkeeping (STCW) by the International Maritime Organization in 1995, using engine room simulators (ERSs) has become mandatory in maritime education and training [1]. Maritime institutions worldwide employ ERS for training purposes at both operational and management levels, as outlined in this standard document [2-4]. The first section of this study provides a background on the use of an ERS to demonstrate the level of acceptance of this mandatory training tool in maritime institutions and introduces the design and analysis of a propulsion system for a maritime simulator.

Studies have shown that simulation tools for maritime application and design have yielded positive results [5,6]. However, using ERS in propeller modeling is still uncommon. Martelli and Figari [7] conducted a similar study; they designed and modeled the propulsion system of a warship and compared the findings with sea-trial data, but did not provide any data on the engine torque and propulsion power relationship. Such resulting data is important for use in the ERSs to reduce the use of computer resources while continuously calculating and presenting the parameters that are based on the dynamically changing affecting conditions.



Address for Correspondence: İsmail Çiçek, İstanbul Technical University Maritime Faculty, Department of Marine Engineering, İstanbul, Türkiye
E-mail: ism@drcicek.com
ORCID ID: orcid.org/0000-0003-4850-1747

Received: 23.11.2022
Last Revision Received: 11.02.2023
Accepted: 22.02.2023

To cite this article: İ. Çiçek, and N. Yılmaz. "Modeling and Analysis of Container-Type Ship's Marine Propeller for Engine Load Conditions." *Journal of ETA Maritime Science*, vol. 11(1), pp. 14-27, 2023.

©Copyright 2023 by the Journal of ETA Maritime Science published by UCTEA Chamber of Marine Engineers

1.1. Engine Room Simulator Applications

There have been numerous publications in the literature on the application of marine engine simulators. For instance, Jianyuan [8] conducted a simulation study on a 6-cylinder, Maschinenfabrik Augsburg-Nürnberg AG (MAN) marine diesel engine, comparing the results with data obtained from the same type of engine. Theotokatos [9] employed two different simulation approaches to study a 9-cylinder MAN-type marine diesel engine and compared the results of both approaches. ERS is mainly designed to train engineering cadets for operational and management level competencies, as specified in IMO STCW 2010 [10]. IMO Model Course 2.017 [11] also outlines the exercises necessary to achieve these competencies. Simulator-based training offers several advantages in the field of marine engineering and technology. ERS has been recognized as a valuable tool for training and evaluating seafarers [12]. Academic publications also contribute to improving ERS exercises and offer a comprehensive understanding of how ERS can be employed in various design, training, and educational studies. Mangga et al. [13] showed how ERS could be used to assess the performance of students. Zaini [14] studied the effectiveness of ERS as a learning tool in maritime education and training. Chybowski et al. [15] provided several examples of ERS usage as a tool for explosion and fire prevention training. Kojima et al. [16] designed ERS scenarios for engine room resource management training, while Kluj [17] emphasized the importance of the environmental awareness concepts in ERS training. In addition to being mandatory in accordance with international agreements [10], the wide range of publications are available on ERS demonstrating its acceptance as a tool for maritime education and training worldwide. This is further evidenced by the fact that a Google Scholar search for the keywords “Engine Room Simulator” and “Training” yielded 220 results related to the topic.

Another area in which simulators are used is in understanding the behavior and performance of ship engines, propulsion systems, and in the design and demonstration of models and analysis studies. Seddiek [18] examined engine performance and simulated various processes to demonstrate how ship performance and energy management could be improved. Seddiek's [18] findings demonstrated that emissions and fuel consumption could be reduced using different operational methods. Yutuc [19] studied the overall efficiency of ships by incorporating a shaft generator. There are also publications detailing the partial or complete development of ERS. Weifeng et al. [20] designed a model to simulate a hydraulic steering gear system. Shen et al. [21] presented an educational virtual

reality training system that enables students to understand the working principle of marine engineering systems and enhance their practical ability skills more efficiently. Rubio et al. [22] developed and presented a marine diesel engine failure simulator based on a thermodynamic model. Jung et al. [23] generally described the development of a marine ERS for use in training and research.

1.2. Engine Room Simulator and Propulsion

The aforementioned publications were presented as examples of ERS development; however, the authors of this study could not find a publication on the development of an ERS that describes the propulsion system design and analysis and how propulsion modeling has been introduced in an engine room training simulator. Although the field of propulsion systems studies is extensive, there is a lack of information regarding the integration of analysis results into ERS. When developing simulators, propulsion parameters must be estimated using either a modeling and analysis approach or test data that can be correlated to match the simulation algorithms. For instance, Altosole and Figari [24] developed a propeller system simulation using the torque and power parameters of the main engine. Karlsen [25] modeled a propulsion system for control system development. Özsari [26] conducted a thermodynamic performance analysis for a submarine propulsion system. Similarly, Chavez et al. [27] modeled three propulsion systems for a fishing vessel to model and simulate the Sunkey diagram. In this study, the method to develop a propeller and analyze the propulsion system for the engine load conditions with respect to each of the speed, or revolutions per minute (RPM), which was employed for a containership, as described in Section 2 Methodology.

1.3. Modeling & Analysis of Ship Propulsion Systems

The analysis and modeling of a ship's propulsion system are crucial in determining the performance, reliability, and efficiency of ships in shipping operations. The primary components of the propulsion system, propellers, can be modeled and analyzed using various methods, including lifting line, lifting surface, and Computational Fluid Dynamics (CFD) approaches [28]. Although in the past, numerical approaches such as lifting surface and boundary element approaches have been preferred for propeller design and hydrodynamic performance computations of marine propellers, CFD approaches have become more common due to the recent technology developments with high computer performance capacities.

Numerous publications have reported the analysis of marine propellers using CFD computations. Rhee and Joshi [29] simulated the flow around a marine propeller using the Reynolds-averaged Navier-Stokes equations (RANS

equations) and compared the CFD findings with experiments, showing good agreement in terms of propeller thrust and torque values. Kulczyk et al. [30] examined a David Taylor Model Test Basin (DTMB) standard propeller using the RANS approach with $k-\epsilon$ and $k-\omega$ turbulence models. Wang et al. [31] conducted another RANS computation with a ship model consisting of twin rotating propellers and turning rudders during zig-zag maneuver. Brizzolara et al. [32] conducted a systematic comparison of the hydrodynamic analysis of a propeller using RANS and panel approaches. Bertetta et al. [33] simulated the Contracted Loaded Tip propeller using the potential panel approach and a RANS solver to predict propeller performance. Bertetta et al. [34] also presented a new design method based on a coupling approach between a panel code and an optimization algorithm to design a controllable pitch type propeller at different pitch angles. The new method aimed to reduce the propeller cavitation and correspondingly underwater radiated noise.

The CFD approaches are generally employed to predict propeller performance in cavitating conditions, although the hydrodynamic simulations in this study were conducted in non-cavitating conditions. For instance, Morgut and Nobile [35] performed CFD simulations with two model scale propellers to predict propeller performance in cavitating conditions using three different cavitation models. Gaggero et al. [36] presented a propeller design method, including reliable numerical computations with RANS model to predict the tip and tip leakage vortex cavitation for two ducted and one conventional propeller. Recently, Shora et al. [37] conducted simulations of a marine propeller with different geometrical and physical parameters using CFD methods to predict hydrodynamic performance. ERS typically uses the analysis results of the governing equations that represent the models of propulsion systems. Using the modeling, optimization studies are performed for research studies such as propulsion performance [38]. Piaggio et al. [39] modeled a propeller for an escort tug for a maneuverability model and simulation. However, the aim of this study was different from that defined in these publications. In this study, a maritime propeller was modeled and analyzed to obtain the thrust and torque relationship with different propeller parameters to use the resulting data in developing a new simulation.

1.4. Scope of the Study

In the scope of this study, CFD analyses of a marine propeller were conducted using the data from an existing marine ERS, which was developed by Kongsberg Norcontrol AS, located at the Istanbul Technical University Maritime Faculty (ITUMF) campus, and is currently employed in the education and training of marine engineering students and maritime

personnel. The development of these types of simulators is crucial for educating new members in the maritime sector. In this respect, the primary aim of this study is to design a more efficient propeller than the existing one to predict the performance parameters and develop a new propulsion system to be employed in developing a new ERS.

The authors of this study designed a new propeller using the trust requirements for a specific ship and obtained the propulsion data using CFD analysis. This study's novelty is to design a more efficient propeller for a newly developed ERS using the CFD approach for a better understanding of the dynamics of the propulsion system and using it to explain the new cadets more professionally.

Within the framework of the above introduction and main objective, this study focuses on a more efficient propeller design than the propeller operating in an existing ERS, simulating the hydrodynamic performance of the propeller, and comparing the CFD simulation results with the simulator's outputs. Furthermore, this study presents the design procedure of a marine propeller using ERS data as inputs. The paper continues with the presentation of an approach that has been used in this study, including the general approach and the process at §2. The propeller design procedure has been presented in §3, including ship resistance computations, propeller initial design, and propeller's parameters. The details and the findings of CFD simulations for the propeller geometry in various operating conditions have been demonstrated in §4. Finally, the study concludes with remarks and discussions in §5, presenting the propulsion data obtained for use in modeling and simulation of the propulsion system in the ERS.

The authors' simulator modeling based on propulsion system analysis is the first publication of its kind, providing a detailed demonstration of how to obtain model data. The presented data and methodology can be used by simulator developers in their developmental studies.

2. Methodology

2.1. General Approach

A custom propeller was modeled and examined for a large container ship. The analysis considered the maneuvering modes of the engine, which were obtained from the existing ERS, as described in §1. Figure 1 illustrates the conceptual application of the propeller to be employed in a ship propulsion system with the maneuvering modes of the engine. In this study, the maneuvering modes are called the operational modes of the engine with respect to its speed in RPM. Thus, in practice, these modes are called RPM modes. These modes are called the engine's RPM modes in this study. In these modes, the engine has predefined speed values. The RPM modes create boundary conditions in

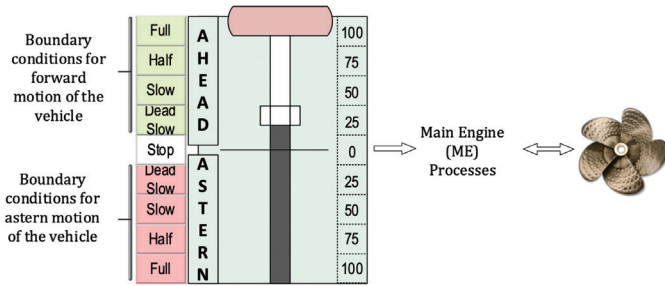


Figure 1. Conceptual view of propeller analyses with respect to the RPM modes of the main propulsion engine

terms of the load or resistance that develops with respect to the speed of the propeller. The performance of the designed propeller was analyzed for each of these RPM modes.

This study explains the modeling and development process of a marine propeller. The author’s primary interest is to design a new propeller model and simulate its hydrodynamic performance employing CFD approaches and obtain well-structured parametric data for use in simulator development. A simulation platform development effort has been continuing in parallel to this study, which is planned to be published at a later date. The simulator called the ship ERS will be used in the training of marine engineering cadets. In such simulations, all systems of the ship’s engines and systems must run interactively and be displayed in real-like gauges and indicators at different ship speeds. In such environments, the aim is not to conduct continuous analysis but to display and change parameters dynamically at a relatively fast rate. Thus, the authors performed analysis for each mode of the engine’s RPM modes and established a matrix of the outputs representing the ship’s propulsion parameters, to effectively use the results in the operation of the simulator.

The ship dimensions and the general characteristics were selected from the existing simulator employed in this study (Table 1). This simulator was used in the training of marine engineering cadets since 2003 by the ITUMF ERS lecturers. In this study, this simulator is called “Existing Simulator” and the simulator where the output data will be used is called “Future Simulator” for distinguishing from each other.

2.2. Process

The first step of this process is to identify the ship and its operational and environmental conditions, as shown in Table 1. Figure 2 illustrates the overall methodology and procedure of modeling and analysis of a propeller obtaining data to use in the simulator application. The process demonstrates the iterative improvement in the propeller design employing the CFD analysis findings and can be listed, in respective order, as follows:

Table 1. General characteristics of the ship

Specifications	Value	Unit
Type	Container	
Cruise speed	25	knots
Length	295.00	m
Width (B)	32.00	m
Draft (T)	12.60	m
Displacement	5500/93500	TEU*/ton
Engine power	48600	kW
Engine speed (@ Navigation full/cruise speed)	102	RPM

*TEU: Twenty-foot equivalent unit

- Develop specifications (Sec 2.1),
- Compute ship resistance and obtain power-speed data (Sec 3.1),
- Obtain propulsion requirements (Sec 3.2.1),
- Propeller design (Sec 3.2.2),
- Perform CFD analysis (Sec 4),
- Compare performances of new and existing propellers (Sec 5),
- Provide propeller performance data for the new propeller design (Sec 5).

3. Propeller Design

3.1. Ship Resistance

Before the propeller design process, the total resistance and power requirements of the ship must be computed under various operational conditions and ship speeds. For this purpose, first, the total ship resistance, R_p , was computed using various ship speeds, with Maxsurf software and a MATLAB code, for finding the power requirements for the propulsion. Figure 2 demonstrates the force equilibrium of forces due to the ship’s speed in a forward direction.

Figure 2 illustrates the changing power requirements due to the losses of the propulsion system, where P_E , P_B , P_D , and P_T represent effective power, engine brake power, propeller-delivered power, and propulsion power, respectively. V

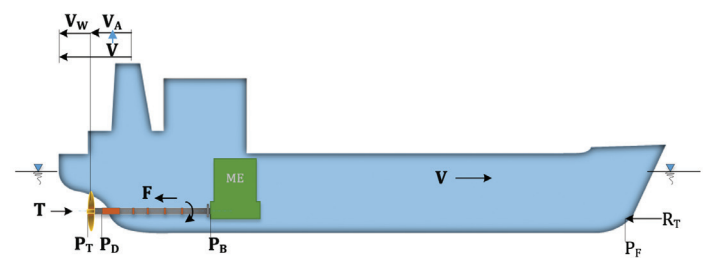


Figure 2. A conceptual drawing for modeling the ship’s power and resistance relations

represents the ship's speed and VA represents the advanced speed of the propeller. R_T represents the total resistance of the ship.

The ship's resistance can be computed using the following equation:

$$R_T = R_W + R_F + R_{VP} \quad (1)$$

where R_W , R_F , and R_{VP} represent wave making, friction, and viscous pressure resistances, respectively. Maxsurf HullSpeed module, which uses the Holtrop-Mennen approach, was employed for computing the total resistance and the required propulsion force [40]. Furthermore, a MATLAB code was developed to compute the total resistance of the ship, and the findings were also compared with Maxsurf computations in Figure 3.

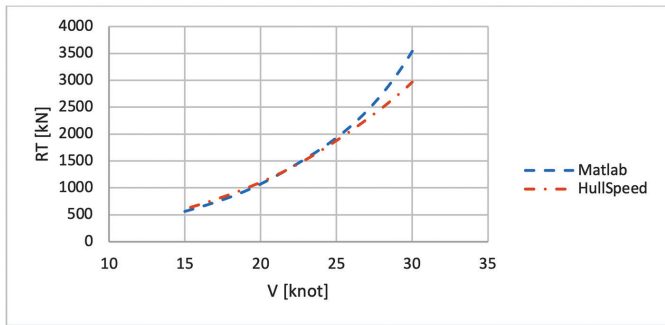


Figure 3. Ship resistance data obtained using MATLAB Code and Maxsurf

The total resistance of the ship was computed using various ship speeds within the operational range of the ship: 15-30 knots in both computations. The findings are plotted and illustrated in Figure 3, including the comparison between Hullspeed and MATLAB results. The findings were very close up to 25 knots ship speed; however, there was a noticeable difference above 25 knots. Although the same numerical method [40] was employed for both computations, the deviations between these two approaches can be explained by geometrical effects. While the HullSpeed module employs a three-dimensional (3D) ship model, the MATLAB code uses the main dimensions of the ship to compute the total resistance of the ship, which affects the computation of the total resistance. The discrepancy for higher velocity can be explained as a reason for these different inputs for the computations. The findings demonstrate that the MATLAB code can offer very close results for this case within the operational speed ranges. It was in the authors' special interest that the MATLAB code was developed to validate and employ in the parametric simulator development. Using this code, ship speed, resistance, and power requirements for different ship sizes can be determined without an external code in the simulator program.

The power requirements of the ship were also obtained from the Maxsurf HullSpeed program, including ship speed against power. In this section of the study, the power requirement was around 44000 [kW] for achieving the cruise speed of the ship (25 knots), which is the same power specification that is obtained from the simulator.

3.2. Propeller Initial Design

3.2.1. Propulsion requirement

The authors employed the mathematical modeling approach for describing the relationship between the total resistance and propeller thrust due to the lack of the model ship test data. Wake fraction, w and thrust deduction, t can be computed using the equations as follow [41] :

$$w = 0,5 * C_B - 0,05, \quad (2)$$

$$t = 0,058 + 0,188 * C_B, \quad (3)$$

where C_B represents the block coefficient of the vessel.

Using Equations 2 and 3, wake fraction (w) and thrust deduction (t) was computed to be 0.198 and 0.151, respectively.

The relationship between the propeller thrust and ship resistance can be computed using the following equation [28]:

$$T_P = \frac{R_T}{n_{propeller} * (1 - t)} \quad (4)$$

where T_p represents the propeller thrust and n represents the revolution speed of the propeller. All symbols employed in this study's computations are defined in Table 2 to ease the readability of the manuscript.

For a cruise ship speed of 25 knots, using the ship's resistance at this speed obtained from Figure 3 and inserting n and t into Equation 4, propeller thrust to use in the propeller design, was found as $T_p = 2238.527$ kN. Using the resistance and thrust requirements of the propeller shown in previous sections, the findings were compared to the characteristics of the main diesel engine employed in the existing ERS (Table 3).

The torque limit of the engine can be computed as follows:

$$P_B = 2 * \pi * Q * n \quad (5)$$

or

$$Q = \frac{P_B}{2 * \pi * n} \quad (6)$$

where P_B , Q , and n represent the engine brake power, torque, and revolution speed of the propeller, respectively. The engine is directly coupled to the propeller without a reduction gear. Using Equation 6, the torque was computed for the power at cruise speed as 4552.26 kNm. Assuming the shaft efficiency of 95%, the torque would be 4324.65

kNm with 46170 kW of the transmitted power to the propeller.

3.2.2. Propeller initial design

Although there are several parameters for developing a custom propeller for a ship, the main propellers design parameters such as diameter, pitch ratio, number of blades, expanded area ratio (EAR), skewness, rake, thickness, blade section profile, and material type are considered in

Table 2. Nomenclature

Symbol	Meaning	Symbol	Meaning
L	Length (m)	P_T	Propulsion Power (kW)
B	Breadth (m)	P_E	Effective Power (kW)
T	Draught (m)	w	Wake Fraction (-)
V	Velocity (m/s)	t	Thrust Deduction (-)
V_A	Advanced Velocity (m/s)	C_B	Block Coefficient (-)
F	Force (kN)	n	Revolution Rate (rps/rpm)
T	Thrust (kN)	n	Propeller Blade Number (-)
T_p	Propeller Thrust (kN)	A_E	Expanded Area (m ²)
Q	Torque (kNm)	A_o	Propeller Disc Area (m ²)
R_T	Total Resistance (kN)	Z	Propeller Blade Number (-)
R_w	Wave Making Resist. (kN)	P_0	Static Pressure (N/m ²)
R_f	Frictional Resistance (kN)	D	Propeller Diameter (m)
R_{vp}	Viscous Press. Resist. (kN)	P_v	Saturation Pressure (N/m ²)
P	Pitch	x	Dist. between shaft and hull (m)
P/D	Pitch to Diameter Ratio (-)	J	Advance Ratio (-)
s	Propeller Slip	K_T	Thrust Coefficient (-)
P_B	Break Power (kW)	K_Q	Torque Coefficient (-)
P_D	Delivered Power (kW)	η_0	Open Water Propeller Eff. (-)

Table 3. Propulsion engine (main diesel engine), Sulzer RTA 84C, characteristics

Specifications	Value	Unit
Cylinder diameter (bore)	84	[cm]
Piston stroke	240	[cm]
Number of cylinders	12	[-]
MCR	48600	[kW]
Engine speed	102	[rpm]
Fuel consumption	171	[g/kWh]

this study. The following paragraphs explain the design considerations made for each of these parameters.

3.2.3. Propeller diameter (D) and number of blades (N)

The propeller thrust must be maximized to have the maximum propulsion power, which is converted from the engine brake power most efficiently by the propeller. Thus, the propeller diameter can be selected to be close to the maximum [28], considering the minimum clearance between the tip of the propeller and the hull structure.

Using the guidance of the [42] publication, the clearance between the hull structure and propeller tip and maximum diameter was computed as follows:

$$\text{Propeller clearance} = \frac{25 * x}{75} \quad (7)$$

where x represents the distance between the shaft and hull structure above the propeller's centerline, which is around 5.9 m, using the 3D ship model, which was modeled in this study. Thus, the required clearance and the maximum propeller diameters were computed as 1.9 m and 7.8 m, respectively. Considering the operational needs explained in the above paragraphs and the maximum propeller clearance obtained using Equation 7, the diameter, D, was selected as 7.8 m.

The propeller for this type of ship is assumed to have number of blades between 2 and 6. The propeller efficiency could be higher as the number of blades selected is minimum, while the mechanical loads on each blade would be higher. Thus, propellers for high-pressure operation and high propulsion load requirements are usually selected to have more than four blades. Since the ship propulsion loads would be very high for this ship type (Table 1), the number of blades, N, selected for this ship was 5. In optimization studies, the recommendation is to repeat the modeling and analysis of various numbers of blades to determine the most suitable number of blades for a specific application.

3.2.4. EAR and pitch ratio (P/D)

The ratio of EAR to blade area, of 0.55 is commonly accepted to be ideal. The pitch (P) is computed using the propeller slip (s) in the water [28], as follows:

$$P = \frac{V}{(1-s)*n} \quad (8)$$

With ship speed of 25 knots and a propeller revolution speed of 102 rpm, as well as a slip rate of the propeller of 0.15, using Equation 8, P was computed to be 8.9 m, which yields a ratio of P/D of 1.14.

For computing EAR, Keller cavitation criterion [43], which is represented by Equation 9, were used as the initial method for identifying the cavitation.

$$\frac{A_E}{A_0} = \frac{(1,3+0,3*Z)*T_p}{(P_0-P_v)*D^2} + k \quad (9)$$

where,

A_E represents the expanded area

A_0 represents the propeller disc area

Z represents the number of blades

T_p represents the propeller thrust [N]

P_0 represents the static pressure at the propeller centerline [N/m²]

D represents the propeller diameter [m]

P_v represents the saturation (vapor) pressure (~1700 [N/m²])

and k is a coefficient determined by the ship type, speed, and the number of propellers. For slow-speed cargo ships, k is used as 0.1 [43].

The thrust power, T_p , was entered from the result of Equation (4) as 2238.527 kN. Using $P_0 = P_{atm} + \rho gh_s$, P_0 , the pressure on the centerline of the propeller was computed as 174326.115 [Pa]. The dimensionless EAR parameter value in this study was considered to be 0.7 because this number should be smaller than that found using Keller's formula.

3.2.5. Propeller geometry

The propeller initial model was established employing the Wageningen propeller series [44]. In later sections of this study, the authors present the changes made to this initial model after evaluating the findings obtained in the CFD analysis. The blade geometry was developed in a propeller design application considering an EAR value of 0.7 and the pitch values are obtained using the lifting line approach. Table 4 displays the design parameters and Figure 4

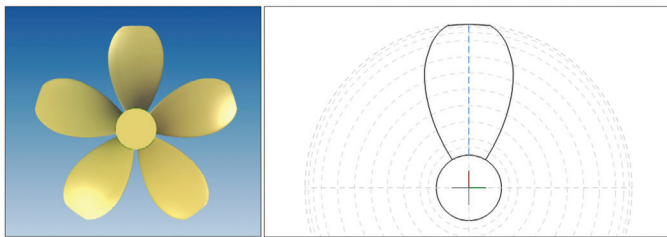


Figure 4. Initial propeller design and 2-D projection of the blade

Table 4. Initial propeller design parameters

Parameter	Value	Unit
Number of blades	5	[-]
Diameter	7.8	[m]
Propeller shaft diameter	1.560	[m]
Extended area ratio	0.702	[-]
Average pitch	9.013	[m]
Average pitch ratio	1.156	[-]

illustrates the 3-dimensional initial propeller and two dimensional projection of the blade model developed and used in the analysis.

Blade section profiles were selected using a = 0.8 Mean Line (mod) and National Advisory Committee for Aeronautics 66 (mod) used for the thickness profile.

The blade thicknesses associated with various blade diameters were computed using the rules and guides provided by the Turkish Lloyd (TL) Class organization [45]. Using TL guides, the propeller material was selected is a copper-manganese-aluminum alloy, commonly known as CU4 type, with a tensile strength of 630 N/mm². The thickness criteria using the TL guides offer the following information for different radii: For 0.25xR, $t \geq 367.31$, for 0.35xR, $t \geq 306.20$, and for 0.6xR, $t \geq 207.03$.

4. CFD Analysis of the Propeller

4.1. Validation and Verification Studies with Standard Test Propellers

CFD simulations were performed on the new propeller design for a container ship to obtain data for use in an ERS development study. However, before this, the authors analyzed two standard test propellers, Potsdam Propeller Test Case (PPTC) Validation Propeller (VP) 1304 and DTMB 4119 using the RANS method with ANSYS Fluent to validate the CFD environment (Figure 5). The findings of the analyses of the standard propellers were compared with published studies for justification. This subsection briefly summarizes this part of the verification analysis using CFD, and Sections 4.2 through 4.6 provide details of the CFD analysis conducted for the newly designed propeller.

Several researchers [30,32,46,47] have tested and simulated these standard test propellers using experimental fluid dynamics (EFD) approaches. The findings have also been presented in the open literature for validation and verification purposes. In this study, open-water propeller performance findings that have been measured and computed with experiments in the past were used to compare with the CFD simulation findings.

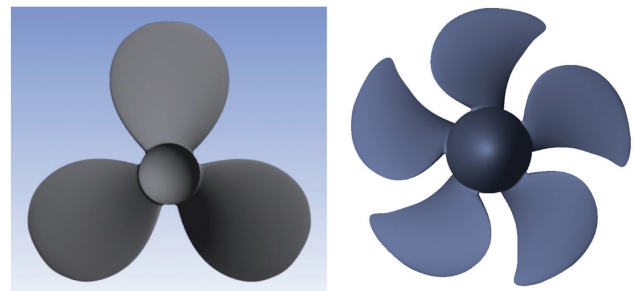


Figure 5. Validation studies with standard test propellers (left: DTMB 4119, right: PPTC VP 1304)

For the validation studies, the standard test propellers were simulated with only one blade configuration to reduce the generated mesh and solution time. The moving reference frame method was used to describe the rotation of the flow domain around the propeller blade. The RANS $k-\omega$ model was preferred for modeling turbulence in the open-water calculations. Suitable meshes were generated for each propeller case, as illustrated in Figure 6.

The CFD findings for the DTMB 4119 and PPTC VP 1304 propellers were compared with the experiments published in the open literature [30] and [46], respectively, in terms of propeller performance coefficients (K_T , $10K_Q$, and n_0).

Table 5 displays the comparisons of the propeller performance coefficient between the CFD and EFD results for the DTMB 4119 standard test propeller. The CFD findings showed a deviation of 3% from the experiments. The comparison revealed good agreement not only for propeller performance coefficients but also for the velocity distribution behind the propeller and pressure distribution on propeller surfaces.

Table 5 displays the comparison of the propeller performance coefficient between CFD and EFD results for the PPTC VP 1304 standard test propeller. The CFD findings demonstrated good agreement with the experiments, with

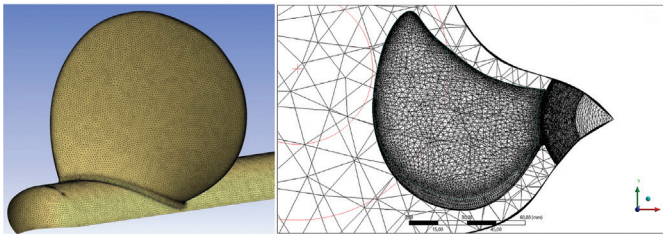


Figure 6. Generated mesh for one blade (Left: DTMB 4119, Right: PPTC VP 1304)

DTMB: David Taylor Model Test Basin, PPTC: Potsdam Propeller Test Case, VP: Validation Propeller

a deviation of less than 3%, similar to the findings for the DTMB 4119 propeller CFD findings.

These validation studies conducted on DTMB 4119 and PPTC VP 1304 standard test propellers confirm that the CFD approach with one-blade analysis, generated mesh, and turbulence model produces highly accurate results for predicting open-water propeller performance. The authors have previously published more detailed results of these validation and verification studies for both propellers [46].

After the validation studies for two different standard test propellers, the same CFD simulation approach was used to analyze the new propeller design for a container ship, which will be employed to develop a new ERS. The analysis approach employed for the new propeller design is presented in detail in the following sections.

4.2. Analysis with Computational Fluid Dynamics

The CFD analysis was iteratively conducted using ANSYS Fluent. The propeller performance and efficiency were estimated for each engine RPM modes. Input parameters for CFD simulations were defined for each gear lever position based on simulator outputs. The inputs such as the propeller revolution speed and the expected ship velocity were specified from the ERS for use in CFD computations. The CFD findings, which are thrust and torque values were compared with the existing simulator data. The CFD analyses were simulated for each engine RPM Mode (Figure 1) and presented in Table 6.

4.3. CFD Model, Input Data, and Setup

The flow domain was prepared around propeller geometry employing the Design Modeler module of ANSYS. To compute the propeller performance, only one blade was simulated, which reduced the number of mesh and computation time required for the analysis. The flow domain was modeled around the propeller geometry as a

Table 5. DTMB 4119 Propeller performance coefficient comparisons between CFD and EFD

	J [-]	V_A [m/s]	n [1/s]	K_T [-]	$10K_Q$ [-]	n_0 [-]
CFD results	0.833	4.5701	18	0.1442	0.273	70%
EFD results	0.833	4.5701	18	0.1460	0.28	69%
Deviation (CFD-EFD)	-	-	-	-2%	1%	-3%

CFD: Computational fluid dynamics, EFD: Experimental fluid dynamics

Table 6. PPTC VP 1304 Propeller performance coefficient comparisons between CFD and EFD

	J [-]	VA [m/s]	n [1/s]	KT [-]	$10K_Q$ [-]	n_0 [-]
CFD results	0.6	2.25	15	0.6159	1.4098	41%
EFD results	0.6	2.25	15	0.6288	1.3964	43%
Deviation (CFD-EFD)	-	-	-	-2	1	-3

CFD: Computational fluid dynamics, EFD: Experimental fluid dynamics, PPTC: Potsdam Propeller Test Case, VP: Validation Propeller

rotating domain using the MRF technique to describe the rotational motion. A suitable mesh structure was generated using tetrahedral elements in the flow domain with the ANSYS Meshing module. To generate the mesh, the number of elements, skewness, orthogonal quality, and aspect ratio, were 2251466, 0.89, 0.112, and 41.644, respectively.

4.4. Boundary Conditions

Boundary conditions were set for each of the RPM modes for analysis (eight different analysis modes) associated with the engine’s maneuvering modes, in the ahead and astern directions, as illustrated in Table 7. The different boundary conditions were set for the inlet patch position due to the direction of flow (ahead and astern) and have been described in detail in the following sections. To model turbulence, the RANS k- ω SST turbulent model was employed for predicting propeller performance. The density of seawater was set to 1025 kg/m³ for the fluid type for all analyses.

4.4.1. Boundary conditions for the analyses in the ahead RPM modes

During the propeller operation behind the ship, the forward surface of the propeller blade (suction side) facing the upcoming flow was considered the inlet boundary condition, and the back surface (pressure side) was considered the outlet boundary condition for the CFD analyses in the ahead RPM modes. The water flow velocity associated with ship

speeds of 9.16, 14.68, 21.01, and 25 knots, was determined in meter-per-second. The outlet boundary condition was defined as a pressure outlet condition at 0 Pa. The propeller’s blade, hub, and shaft surfaces were described as “no slip wall” boundary conditions. The surface on the outward direction from the flow domain was selected as symmetry. The interface for 1/5 flow volumes was defined as the periodic boundary conditions and described as periodically sequenced in ANSYS Fluent. Figure 7 shows the summary of the boundary conditions depicted on the model for analysis.

4.4.2. Boundary conditions for the analyses in the astern RPM modes

For the analyses in the astern RPM modes, the forward surface of the propeller blade (suction) was considered the outlet side, and the back surface (pressure) was considered the inlet side of the propeller, similar to the analyses in the ahead RPM modes. The boundary conditions used in the analyses of the ahead RPM modes were kept the same for the propeller analyses of the astern RPM modes, except that the positions of the inlet and outlet were changed. A pressure outlet condition of 0 Pa was set at the outlet side of the propeller. The required inflow velocities were also changed to 6.98, 11.68, 14.28, and 19.57 knots of ship speed occurring from ship’s backward directional motion.

Table 7. Gas lever position (RPM modes)

Parameters	Full ahead	Half ahead	Slow ahead	D. slow ahead	D. slow astern	Slow astern	Half astern	Full astern
Ship speed [knots]	25.05	20.01	14.68	9.16	-6.98	-11.68	-14.28	-19.57
Propeller speed [rpm]	102	80.02	58.01	36	-36.03	-55.04	-73.42	-92.11
Propeller power [mW]	42.89	19.72	7.25	1.7	2.27	16.28	19.1	30.58
Propeller thrust [kN]	2490.47	1404.65	691.75	257.03	-418.8	-655.85	-1721.1	-1918.1

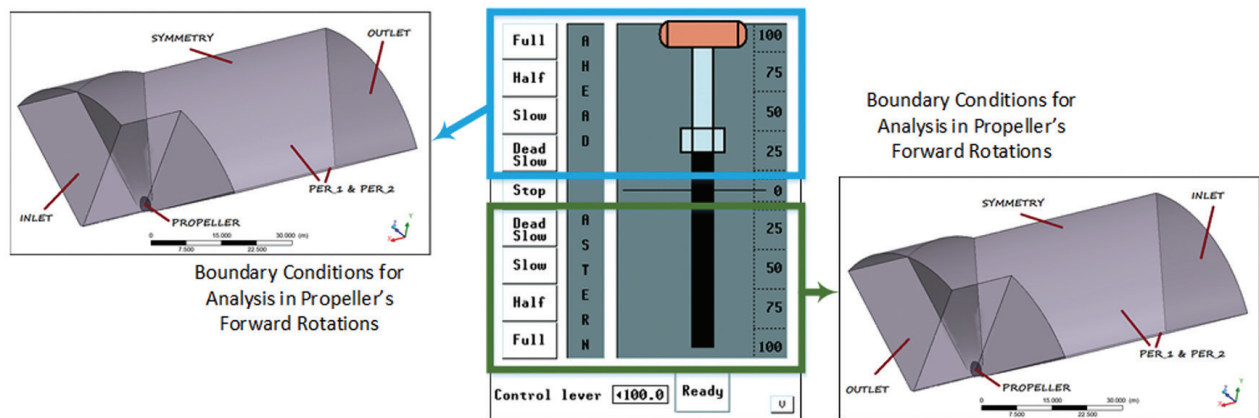


Figure 7. Boundary conditions shown on the propeller model for the analysis in the ahead and astern RPM modes
 RPM: Revolutions per minute

5. Results and Discussion

Analyses for eight RPM modes associated with the engine’s maneuvering modes in ahead and astern directions were conducted to compute the hydrodynamic performance of the propeller (Table 7 and Figure 7). Figure 8 illustrates the flow velocity distributions behind the propeller blades and shows the pressure distributions on the propeller surfaces. These distributions demonstrated in Figure 8 represent the analysis for one of the ahead RPM modes, provided as an example.

Table 8 displays the comparisons of the propeller performance coefficient for existing and new design propellers for ahead RPM modes. The data demonstrate that the open-water propeller efficiency increased by about 5%-9% with the new propeller.

When compared with the existing simulator data, the new propeller demonstrated a little more thrust in the ahead RPM modes (Figure 9a) and lower power requirements at the same modes (Figure 9b).

Table 9 shows the input parameters, such as ship speed (V_s), propeller speed (V_p), advance velocity ratio (J), propeller’s rotational speed (n), as well the outputs, including propeller

thrust (V_p), torque (Q), and computed performance parameters, thrust coefficient (K_T), torque coefficient ($10K_Q$) and open-water propeller efficiency (n_p). The data from Table 9 and Figure 10 were used to model and simulate the propulsion system. The novelty of this study is the development of a propulsion modeling process for a new ERS application. Figure 10 illustrates a screen capture of the Graphical User Interface (GUI) for the Propulsion System panel employed in the new simulator. Parametric modeling enabled the simulator to alter propulsion parameters, including meteorological ones that affect propulsion

Table 8. Propeller efficiency comparison between existing and new design

Propeller	Performance coefficients	Ahead 100	Ahead 75	Ahead 50	Ahead 25
New design	K_T	0.233	0.225	0.220	0.217
	$10K_Q$	0.445	0.434	0.428	0.425
	n_p	65%	65%	66%	66%
Existing design	K_T	0.227	0.208	0.195	0.188
	$10K_Q$	0.469	0.447	0.431	0.423
	n_p	60%	59%	58%	57%

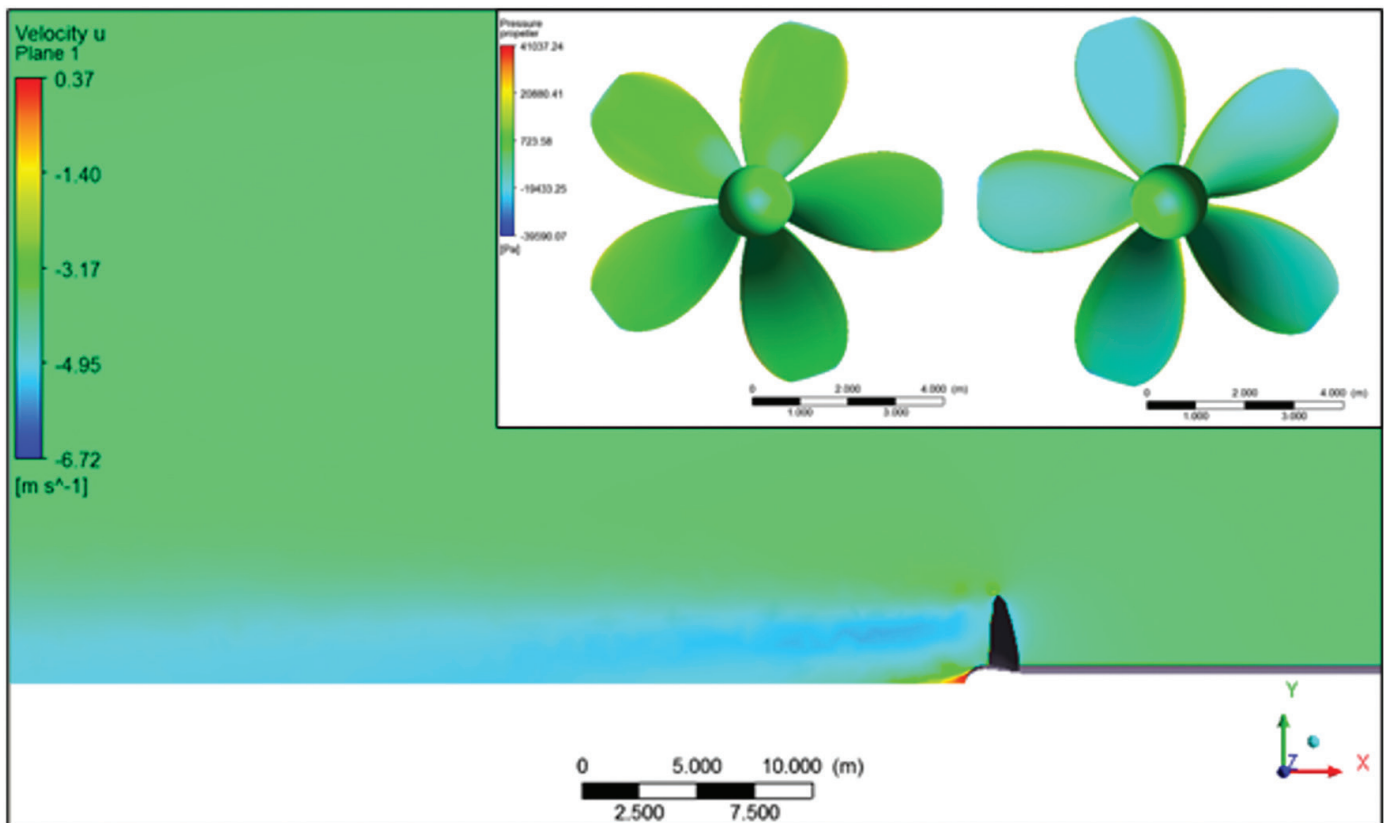


Figure 8. Velocity distribution behind the propeller and pressure distributions on the propeller surfaces for ahead RPM modes of analyses (left: pressure side, right; suction side)

RPM: Revolutions per minute

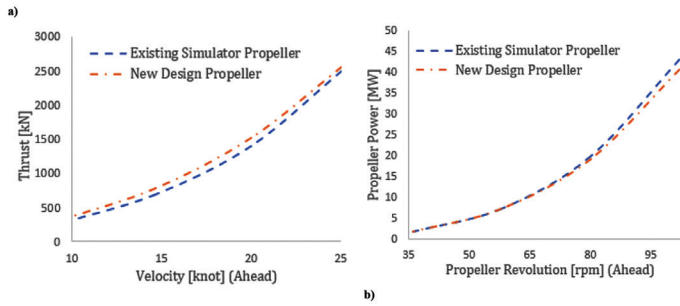


Figure 9. Comparison of ship speed and propulsion a) force, and b) power in ahead RPM modes
RPM: Revolutions per minute

performance. The parametric simulation programming also facilitated the implementation of student exercises, such as propeller slip rate and similar ones described in IMO Model Course 2.07 [8].

6. Conclusion

This study introduces a new propeller design and CFD analysis to obtain propulsion data, which be used to develop a training simulator. To this end, the study has successfully achieved the following.

- Ship resistance computations were conducted using Maxsurf Hullspeed software and MATLAB code with the

Table 9. CFD analysis results

	RPM modes	Ship vel. (V _S)	Adv. vel. (V _A)	Adv. ratio (J)	Rev. (n)	Thrust (T)	Torque (Q)	Thrust coeff. (K _r)	Torque coeff. 10K _Q	Open water eff. (η _o)	Delivered power (P _D)
		[knot]	[m/s]	[-]	[rpm]	[kN]	[kNm]	[-]	[-]	[-]	[MW]
Inlet	Ahead 100	25.05	10.33	0.779	102	2554.50	3806.75	0.233	0.445	65%	40.65
	Ahead 75	20.01	8.26	0.793	80	1519.50	2287.65	0.225	0.434	65%	19.16
	Ahead 50	14.68	6.06	0.803	58	780.77	1184.96	0.220	0.428	66%	7.19
	Ahead 25	9.16	3.78	0.807	36	297.04	453.78	0.217	0.425	66%	1.71
Outlet	Astern 25	6.98	2.88	0.614	36	294.98	476.74	0.215	0.446	47%	1.79
	Astern 50	11.68	4.82	0.673	55	579.26	963.41	0.181	0.386	50%	5.55
	Astern 75	14.28	5.89	0.617	73	1216.81	1958.08	0.214	0.441	48%	15.05
	Astern 100	19.57	8.07	0.674	92	1616.36	2678.8	0.180	0.384	51%	25.83

CFD: Computational fluid dynamics, RPM: Revolutions per minute

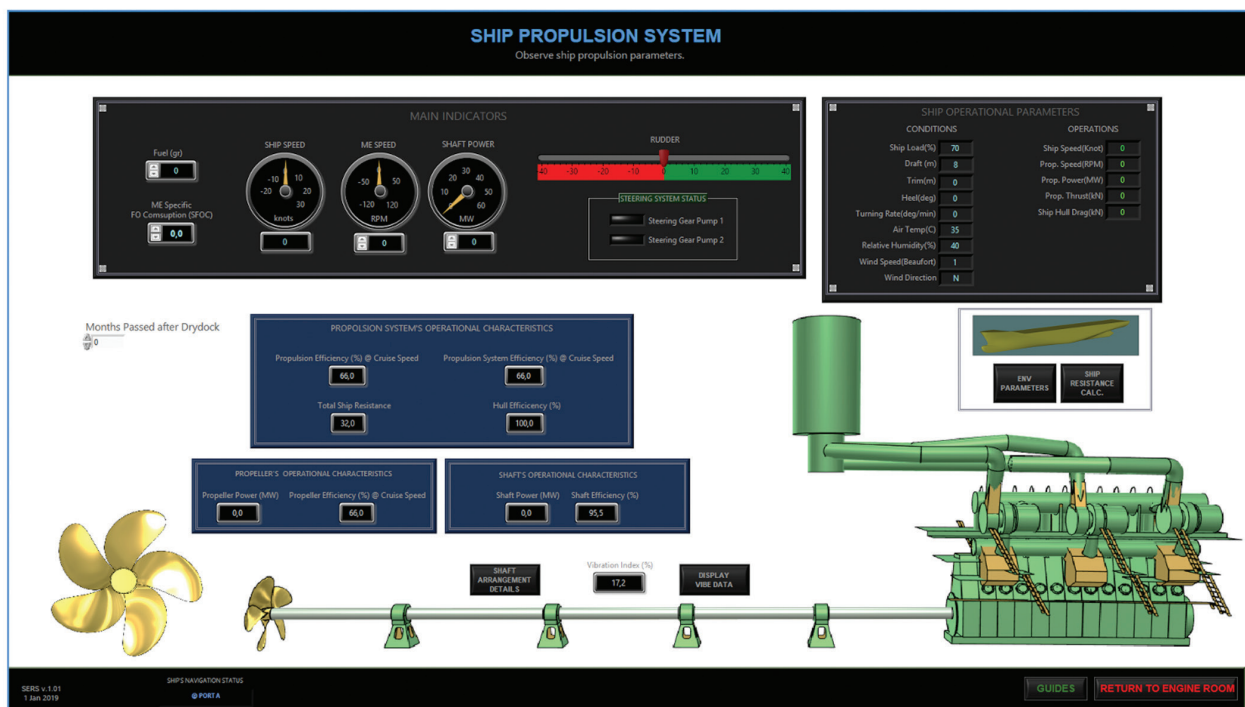


Figure 10. Ship Propulsion System GUI Window captured from the new simulator, which is developed using the data from this study

Holtrop-Mennen method to determine the hull resistance and thrust requirements of the propeller.

- A new propeller was designed based on the propulsion requirements of the simulated ship.
- Validation investigations were conducted using two standard test propellers (DTMB 4119 and PPTC VP 1304) before performing CFD computations for a new propeller design and validating the CFD approach employed in this study. The CFD findings were also compared with those in the literature, and a good agreement was achieved.
- The new propeller was simulated using CFD approaches with commercial CFD software, ANSYS Fluent, at different RPM modes of the main propulsion engine.
- The CFD findings of the new design propeller were compared with the findings of the existing propeller that were obtained from the ERS. The comparison demonstrated a good agreement in terms of propeller performance coefficients, particularly for open-water propeller efficiency. The new design offered more thrust with less power requirement than the existing propeller.
- Propulsion data, including the propulsion performance, torque, and efficiency, were constructed.

The model was developed by employing the existing simulator as a test system to obtain the ship propulsion parameters associated with the engine's speed and load characteristics. The data obtained from the existing simulator is representative of a container-type ship with a fixed-pitch propeller. Another investigation study for this case, including uncertainty studies, is also planned as a future study.

The propeller design, developed equations, and performance analysis findings obtained in this study were crucial not only for providing data for modeling but also for enhancing understanding of the propulsion system modeling, developing a new simulator, and educating new cadets in the marine community. Additional research may further improve this study, as follows:

- A non-dimensional form of the equations could be developed and examined so that the resulting matrix could be directly applied to other types of ships with a fixed-pitch propeller.
- Simulator design and development could be described in a future study, including a discussion of the software architectures and education outcomes.

Acknowledgments

The study herein was part of a project funded by the Turkish Republic Ministry of Science, Technology, and Industry.

The project number and title were 0531.STZ.2013-2 "Development of Ship's Main Engine and Propulsion System Simulator." The authors highly appreciate the support received from this funding organization.

Peer-review: Externally and internally peer-reviewed.

Authorship Contributions

Concept design: Data Collection or Processing: Analysis or Interpretation: Literature Review: Writing, Reviewing and Editing: All authors have contributed equally.

Funding: The author(s) received no financial support for the research, authorship, and/or publication of this article.

References

- [1] IMO, "International Convention on Standards of Training, Certification and Watchkeeping for Seafarers (STCW)." Adoption: 7 July 1978; Entry into force: 28 April 1984; Major revisions in 1995., *International Maritime Organization (IMO) Publication*, 2015.
- [2] S. Al-Sharyoufi, "The utilization of engine room simulators for freshmen and career personnel: training and assessment," *World Maritime University Dissertations*, 1996.
- [3] K. Ikenishi, and T. Nakamura, "Study of Efficient Slef Study using the PC-Based Engine Room Simulator," in *The 7th International Conference on Engine Room Simulators*, 2006.
- [4] I. Cicek, "Integration of Marine Engineering Simulators into Maritime Engineering Education," in *The Proceedings of the First General Assembly of The Chamber of Marine Engineers of Turkey*, Istanbul, May 2003.
- [5] B. Piaggio, M. Viviani, M. Martelli, and M. Figari, "The heel influence on ship manoeuvrability: Single and twin-screw surface vessels," *Ocean Engineering*, vol. 266, pp. 112721, Dec 2022.
- [6] C. Chen, L. Zou, Z. Zou, and H. Guo, "Assessment of CFD-Based Ship Maneuvering Predictions Using Different Propeller Modeling Methods," *Journal of Marine Science and Engineering*, vol. 10, pp. 1131, Aug 2022.
- [7] M. Martelli, and M. Figari, "A design framework for combined marine propulsion control systems: From conceptualisation to sea trials validation," *Ocean Engineering*, vol. 254, pp. 111282, June 2022.
- [8] Z. Jianyuan, "Modeling and Simulating of Container Ship's Main Diesel Engine," in *Proceedings of the International Multi Conference of Engineers and Computer Scientists*, Hong Kong, March 2008.
- [9] G. Theotokatos, "On the cycle mean value modelling of a large two-stroke marine diesel engine," *Proceedings of the Institution of Mechanical Engineers, Part M: Journal of Engineering for the Maritime Environment*, vol. 224, pp. 193-205, Sep 2010.
- [10] IMO, "International Convention on Standards of Training, Certification and Watchkeeping for Seafarers (STCW)." Adoption: 7 July 1978; Entry into force: 28 April 1984; Major revisions in 1995 and 2010, *International Maritime Organization (IMO) Publication*, 2010.
- [11] IMO, "IMO Model Course 2.07 Engine Room Simulator," *International Maritime Organization (IMO) Publication*, 2017.

- [12] Ç. Kandemir, and M. Çelik, "A Human Reliability Assessment of Marine Engineering Students through Engine Room Simulator Technology," *Simulation & Gaming*, vol. 52, pp. 635-649, June 2021.
- [13] C. Mangga, P. Tibo-oc, and R. Montaño, "Impact of Engine Room Simulator as a Tool for Training and Assessing BSMARE Student's Performance in Engine Watchkeeping," *Pedagogika-Pedagogy*, vol. 93, 2021.
- [14] Z. Zaini, "The effectiveness of engine room simulator (ERS) as a learning tool in maritime education and training (MET)," *World Maritime University Dissertations*, 2020.
- [15] L. Chybowski, K. Gawdzińska, O. Ślesicki, K. Patejuk, and G. Nowosad, "An engine room simulator as an educational tool for marine engineers relating to explosion and fire prevention of marine diesel engines," *Zeszyty Naukowe Akademii Morskiej w Szczecinie*, vol. 43, pp. 15-21, 2015.
- [16] M. Kojima, S. Horiki, T. Tsukamoto, A. Uchino, A. Ishibashi, and H. Kobayashi, "Concepts of ETM (Engine Room Team Management) for Safety Operation of Ship Engine Power Plant - Suggestion of Scenario Suitable for Competency Evaluation," in *In of the 13th International Conference on Engine Room Simulators*, 2017.
- [17] S. Kluj, "The Environmental Awareness in the Engine Room Simulator Training," in *In of the 13th International Conference on Engine Room Simulators*, 2017.
- [18] I.S. Seddiek, "Viability of using Engine Room Simulators for Evaluation Machinery Performance and Energy Management Onboard Ships," *Intl J Maritime Eng : Trans RINA, The Royal Institution of Naval Architects A-283*, vol. 161, 2019.
- [19] W. Yutuc, "An Investigation on the Overall Efficiency of a Ship with Shaft Generator Using an Engine Room Simulator," in *In Advancement in Emerging Technologies and Engineering Applications*, pp. 255-265, 2020.
- [20] L. Weifeng, S. Caiqin, W. Chuang, L. Guangxing, and X. Bin, "Modeling, Simulation and Application of the Hydraulic Steering Gear System in DMS2016 Marine Engineering Simulator," *In 2017 9th International Conference on Measuring Technology and Mechatronics Automation (ICMTMA)*, pp. 296-299, 2017.
- [21] H. Shen, J. Zhang, B. Yang, and B. Jia, "Development of an educational virtual reality training system for marine engineers," *Computer Applications in Engineering Education*, vol. 27, pp. 580-602, Jan 2019.
- [22] J.A.P. Rubio, F. Vera-García, J.H. Grau, J.M. Cámara, and D.A. Hernandez, "Marine diesel engine failure simulator based on thermodynamic model," *Applied Thermal Engineering*, vol. 144, pp. 982-995, Nov 2018.
- [23] B.G. Jung, M.O. So, P.Y. Eum, S.H. Paek, and C.H. Kim, "Development of the Marine Engine Room Simulator," *Journal of the Korean Society of Marine Engineering*, vol. 31, pp. 872-880, 2007.
- [24] M. Altosole, and M. Figari, "Effective simple methods for numerical modelling of marine engines in ship propulsion control systems design," *Journal of Naval Architecture and Marine Engineering*, vol. 8, pp. 129-147, Dec 2011.
- [25] A.T. Karlsen, "On Modeling of a Ship Propulsion System for Control Purposes," *Institutt for teknisk kybernetikk*, 2012.
- [26] İ. Özşari, "Thermodynamic Performance Analysis of the MESMA System Used as an Air-Independent Propulsion System in Submarines," *GMO Journal of Ship and Marine Technology*, vol. 221, pp. 59-74, June 2022.
- [27] E.S. Chavez, E. Galarza, J. Lulo, Ramos, N.M.V. Acosta, J. Uchuya, and J. Roggero, "Calculation of the Sankey Diagram for Ship Propulsion Plants Using Online Simulators," in *SNAME Maritime Convention*, 2021.
- [28] J.S. Carlton, "Marine Propellers and Propulsion," 2nd Edition ed., USA: Butterworth-Heinemann, 2007.
- [29] S.H. Rhee, and S. Joshi, "CFD Validation for a Marine Propeller Using an Unstructured Mesh Based RANS Method," in *ASME/JSME 2003 4th Joint Fluids Summer Engineering Conference*, Hawaii, 2003.
- [30] J. Kulczyk, Ł. Skraburski, and M. Zawisłak, "Analysis of screw propeller 4119 using the Fluent system," *Archives of Civil and Mechanical Engineering*, vol. 7, pp. 129-137, Dec 2007.
- [31] J. Wang, L. Zou, and D. Wan, "Numerical Simulations of zigzag maneuver of free running ship in waves by RANS-Overset grid method," *Journal of Ocean Engineering*, vol. 162, pp. 55-79, Aug 2018.
- [32] S. Brizzolara, D. Villa, and S. Gaggero, "A systematic comparison between RANS and Panel Methods for Propeller Analysis," in *Proceeding of 8th International Conference on Hydrodynamics (ICH'D'08)*, Nantes, France, 2008.
- [33] D. Bertetta, S. Brizzolara, E. Canepa, and S. Gaggero, "EFD and CFD Characterization of a CLT Propeller," *International Journal of Rotating Machinery*, vol. 2012, pp. 1-22, July 2012.
- [34] D. Bertetta, S. Brizzolara, S. Gaggero, M. Viviani, and L. Salvio, "CPP propeller cavitation and noise optimization at different pitches with panel code and validation by cavitation tunnel measurements," *Ocean Engineering*, vol. 53, pp. 177-195, Oct 2012.
- [35] M. Morgut, and E. Nobile, "Numerical Predictions of Cavitating Flow around model Scale Propellers by CFD and Advanced Model Calibration," *Hindawi Publishing Corporation International Journal of Rotating Machinery*, vol. 2012, pp. 11, 2012.
- [36] S. Gaggero, G. Tani, M. Viviani, and F. Conti, "A study on the numerical prediction of propellers cavitating tip vortex," *Journal of Ocean Engineering*, vol. 92, pp. 137-161, Dec 2014.
- [37] M.M. Shora, H. Ghassemi, and H. Nowruzzi, "Using computational fluid dynamic and artificial neural networks to predict the performance and cavitation volume of a propeller under different geometrical and physical characteristics," *Journal of Marine Engineering & Technology*, vol. 17, pp.59-84, 2018.
- [38] Y. Ichinose, Y. Tahara, T. Takami, A. Kaneko, T. Masui, and D. Arai, "A Study of Multi-Objective Optimization for Propulsion Performance and Cargo Capacity," in *Practical Design of Ships and Other Floating Structures. Proceedings of the 14th International Symposium, PRADS 2019*, September 2019.
- [39] B. Piaggio, M. Viviani, M. Martelli, and M. Figari, "Z-Drive Escort Tug manoeuvrability model and simulation, Part II: A full-scale validation," *Ocean Engineering*, vol. 259, no. 111881, 2022.

-
- [40] J. Holtrop, and G.G.J. Mennen, "An Approximate Power Prediction Method," *International Shipbuilding Progress*, vol. 335, pp. 166-170, 1982.
- [41] J.D. v. Manen, and P.v. Oossanen, "Principles of Naval Architecture Vol II, Chapter V & VI, Resistance and Propulsion," *The Society of Naval Architects and Marine Engineers*, 1988.
- [42] American Bureau Shipping, Guidance Notes on Ship Vibration, Houston, TX: American Bureau Shipping, 2006.
- [43] A. Keller, "Enige aspecten bij het ontwerpen van schepsschroeven," *Schip en Werf*, 33e Jaargang, vol. 24, pp. 658-663, 1966.
- [44] G. Kuiper, "Wageningen Propeller Series," Netherlands: Maritime Research Institute Netherlands, 1992.
- [45] T. Loydu, Propellers. Cilt B Kısım 4 Makina Kuralları, Bölüm 8, Türk Loydu, 2014.
- [46] G. Seil, R. Widjaja, B. Anderson, and P. Brandner, "Computational Analysis of Submarine Propeller Hydrodynamics and Validation Against Experimental Measurement," in *Conference Proceeding UDT Pacific*, Sydney, 2008.
- [47] N. Yilmaz, and I. Cicek, "Verification Of The Computational Fluid Dynamics Analysis Sub-Structure By Standard Test Propeller Analyzes," *Journal of Engineering Sciences and Design*, vol. 6, pp. 681-690, 2017.